

Mesoscopic quantum coherences in cavity QED: Preparation and decoherence monitoring schemes

L. Davidovich,^{*} M. Brune, J. M. Raimond, and S. Haroche

Laboratoire Kastler Brossel,[†] Département de Physique, Ecole Normale Supérieure, 24 rue Lhomond, F-75231 Paris Cedex, France

(Received 18 April 1995)

We present several schemes for preparing and detecting coherent superpositions of classically distinct states of the electromagnetic field in one or two high- Q cavities. These proposals are based on two-atom correlation measurements, to be performed on circular Rydberg atoms interacting dispersively with the cavity fields. Changing the time interval between the two detected atoms allows a monitoring of the decay of quantum coherence due to dissipation.

PACS number(s): 03.65.Bz, 32.80.-t, 42.50.Dv

I. INTRODUCTION

The nonexistence of quantum superpositions at the classical level has been a long-standing problem in quantum mechanics. Schrödinger emphasized this point in his famous “cat paradox” [1]: if one assumes that the usual rules of quantum dynamics are valid up to the macroscopic level, then the existence of quantum interference at the microscopic level necessarily implies that the same phenomenon should occur between distinguishable macroscopic states. Einstein considered as a fundamental problem the “inexistence at the classical level of the majority of states allowed by quantum mechanics,” namely, those involving the coherent superposition of two or more macroscopically separated localized states [2]. Several possibilities have been explored as solutions to this paradox, including the proposal that a small nonlinear term in the Schrödinger equation, although unnoticeable for microscopic phenomena, could eliminate the coherence between macroscopic states, thus transforming the quantum superpositions into statistical mixtures [3]. More recently, the role of dissipation in the disappearance of coherence has been stressed. Decoherence follows from the irreversible coupling of the observed system to the outside world reservoir [4,5]. In this process, the quantum superposition is turned into a statistical mixture, for which all the information on the system can be described in classical terms, so our usual perception of the world is recovered. Furthermore, for macroscopic superpositions, quantum coherence decays much faster than the usual physical observables of the system, its decay time being given by the energy dissipation time divided by a dimensionless number measuring the “separation” between the two parts. The statement that these two parts are macroscopically separated implies that this separation is an extremely large number. Such is the case for biological systems like “cats” made of huge number of molecules. In the simple case mentioned by Einstein [2] of

a particle split into two spatially separated wave packets by a distance d , the dimensionless measure of the separation is $(d/\lambda_{dB})^2$, where λ_{dB} is the particle de Broglie wavelength. For a massive particle at not too low a temperature, this number is huge and the decoherence is for all purposes instantaneous. This would provide an answer to Einstein’s concern: decoherence of macroscopic states would be too fast to be observed. This decoherence process is also at the heart of quantum measurement theory. von Neumann’s collapse postulate [6] introduces two distinct types of evolution in quantum mechanics: the deterministic and unitary evolution associated to the Schrödinger equation, which describes the establishment of a correlation between states of the microscopic system being measured and distinguishable classical states of the macroscopic measurement apparatus (for instance, distinct positions of a pointer); and the probabilistic and irreversible process associated with measurement, which transforms the correlated state into a statistical mixture. This separation of the whole process into two steps has been the object of much debate [3,7,8]; indeed, it would not only imply an intrinsic limitation of quantum mechanics in dealing with classical objects, but it would also pose the problem of drawing the line between the microscopic and the macroscopic worlds.

Several models have been proposed to demonstrate the “superselection rule” which forbids coherent superpositions of macroscopically separated states [4,5,7–9]. The nonobservability of the coherence between the two positions of the pointer has been attributed both to the lack of nonlocal observables with matrix elements between the two corresponding states [10] as well as to the fast decoherence due to dissipation [5,9]. Precisely because of these two reasons the evolution of coherent superpositions of classically distinguishable states towards statistical mixtures has not been monitored experimentally yet: not only is the decoherence time very short, but besides it is necessary to imagine an experiment which would display interference effects between macroscopically distinct states. This has precluded experimental observation so far, in spite of the large number of theoretical proposals of “Schrödinger cats” and mesoscopic coherences in various contexts. Two different kinds of systems have been considered recently. Josephson junctions in various superconducting quantum interference device (SQUID) configurations have been theoretically analyzed by

^{*}Permanent address: Instituto de Fisica, Universidade Federal do Rio de Janeiro, Caixa Postal 68528, RJ 21945-970, Rio de Janeiro, Brazil.

[†]Laboratoire de l’Université Pierre et Marie Curie et de l’ENS, associé au CNRS (URA18).

Leggett [11] and will not be discussed here. In quantum optics, several schemes have been proposed to prepare fields in superpositions of classically distinguishable states [12]. One of the difficulties with these schemes is that they involve traveling fields, which escape at the speed of light from the experimental area, making tests of quantum coherence difficult to achieve, even conceptually. It is possible, however, to build quantum superpositions of mesoscopic states of fields trapped in one or more cavities, which would display decoherence times within observable range. Such proposals must have two essential ingredients: the first one is a scheme to build the coherent superposition. The second one is a method for displaying the interference effects associated with this superposition, thus circumventing the above-mentioned objections on the inexistence of nonlocal operators.

A proposal along these lines was made in Ref. [13] which suggested a simple method to prepare the coherent superposition, but a rather complicated way of displaying the interference effect. We present in this paper the principle of experiments which fulfill the preparation and detection requirements in a simple way, involving only two-atom correlation measurements. In particular, we show how one can build and detect a superposition of coherent states localized simultaneously in one or two macroscopically separated cavities. This system provides also a test of quantum mechanics analogous to those made in connection with Bell's inequalities [14], which can disprove the existence of a local hidden-variable theory, for quantum-correlated states which are classically distinguishable. Furthermore, it is directly related to the quantum measurement problem, in the sense that the presence of a field in one cavity or the other can be associated to two macroscopically distinct positions of a classical pointer. A short account of some of these results has been given in Ref. [15].

Three different experimental configurations are discussed in this paper. The first one, analyzed in Sec. II, leads to the superposition of two coherent states with different phases in a cavity. The second example, presented in Sec. III, involves a quantum switch which can be put in a coherent superposition of an open or "lighted" state (a coherent state inside a cavity) and a closed or "dark" state (vacuum state in the cavity). Finally, we discuss in Sec. IV a configuration consisting of two cavities, which can be prepared in a coherent superposition with one of the cavities "lighted" and the other "dark," thus leading to a non-local state of the field. In all these cases, a detailed analysis is made of the detection process, and of the decoherence produced by dissipation. The three systems considered here are not only experimentally viable, but also lead to exactly soluble models, and therefore to a precise consideration of the dissipation process. Quantum coherence is detected through two-atom correlation measurements, which display the interference between the two different pointer positions, thus allowing us to distinguish between the quantum states and the corresponding classical statistical mixtures. In fact, this method is a realization of a nonlocal measurement. In the two-atom sequence, the first atom produces the coherent superposition of field states, and the second one, which is sensitive to the interference between these classically distinct states, is used to "read" the coherence. Increasing the delay between the two atoms leaves more time for dissipation to act, and therefore

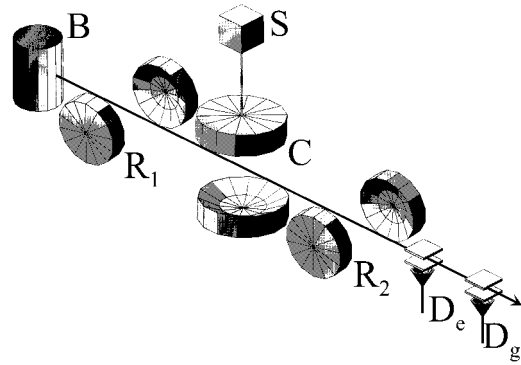


FIG. 1. Experimental arrangement for preparing a superposition of two coherent states with opposite phases in a superconducting cavity.

the coherent effects get smaller in magnitude. One can thus monitor the dynamical effects of dissipation on the superposition state, and follow the transition from the quantum state to the classical mixture. In practice, the rapid decrease of the decoherence time with the intensity of the field in the cavity, the experimental limitations on cavity losses, and the velocity dispersion of the atomic beam lead to an upper limit for the number of photons involved (which should be typically smaller than 100). The experiments described here will involve therefore mesoscopic field states, even though our theory has a wider scope, applying also to truly macroscopic systems.

II. QUANTUM COHERENCE BETWEEN CLASSICAL FIELDS WITH DIFFERENT PHASES

A. Production and detection of the state

We start by briefly reviewing the method presented in Ref. [13] for preparing a coherent superposition of two coherent states [16] with opposite phases in a superconducting cavity. The method, sketched in Fig. 1, involves a beam of circular Rydberg atoms [17] prepared in box *B* and crossing a high-*Q* cavity *C* in which a coherent state is previously injected (this is accomplished by coupling the cavity to a classical source *S* through a waveguide). Circular levels are required because they are strongly coupled to microwaves and they have very long radiative decay times, making them ideally suited for preparing and detecting long-lived correlations between atom and field states. Circular states with principal quantum number *n* around 50 are used in the experiment under way in our laboratory [18]. The radiative lifetime of these levels is 3×10^{-2} s.

The high-*Q* cavity *C* is sandwiched between two low-*Q* cavities (*R*₁ and *R*₂), in which classical microwave fields can be applied. The *R*₁ and *R*₂ set of cavities constitutes the usual experimental arrangement in the Ramsey method of interferometry [18,19]. The transition between two nearby circular atomic states, which we denote by $|e\rangle$ and $|g\rangle$, is resonant with the microwave fields in cavities *R*₁ and *R*₂. To be specific, in the following, $|e\rangle$ and $|g\rangle$ have principal quantum numbers $n=51$ and $n=50$, respectively. The $|e\rangle \rightarrow |g\rangle$ transition frequency is 51.099 GHz. The intensity of the field in *R*₁ is such that, for the selected atomic velocity, a $\pi/2$ pulse is applied to the atom as it crosses *R*₁. Each atom is

prepared in the state $|e\rangle$ in box B . After leaving R_1 it is in a superposition of the two circular Rydberg states $|e\rangle$ and $|g\rangle$ which, with a proper choice of the microwave field phase, is given by

$$|\psi_{\text{atom}}\rangle = \frac{1}{\sqrt{2}}(|e\rangle + |g\rangle). \quad (2.1)$$

The superconducting cavity C is tuned close to resonance with a transition connecting $|e\rangle$ to the circular state $|i\rangle$ (this state corresponds to $n=52$, the frequency of the $|e\rangle \rightarrow |i\rangle$ transition being 48.180 GHz) and is far off resonance with all transitions involving level $|g\rangle$. The cavity mode geometry is such that the field slowly rises and decreases along the atomic trajectory in C , so that, for sufficiently slow atoms, and for large enough detunings, the atom-field evolution is adiabatic. Hence no photon absorption or emission can occur in C . However, dispersive effects can be important. An atom crossing the cavity in state $|e\rangle$ induces an appreciable phase shift on the field in C . Let us assume that this shift can be adjusted to a value exactly equal to π by proper selection of the atomic velocity (of the order of 100 m/s [18]). A coherent field $|\alpha\rangle$ is then transformed into $|-\alpha\rangle$. The phase shift is negligible, however, if the atom crosses the cavity in state $|g\rangle$.

After the atom prepared in the state defined by Eq. (2.1) has crossed the cavity, the state of the combined atom-field system is

$$|\psi_{\text{atom+field}}\rangle = \frac{1}{\sqrt{2}}(|e; -\alpha\rangle + |g; \alpha\rangle). \quad (2.2)$$

Note that the atom crosses the centimeter-sized cavity C in a time of the order of 10^{-4} s, much shorter than the field relaxation time (typically 10^{-3} – 10^{-2} s for a niobium superconducting cavity), and to the atomic radiative damping time (3×10^{-2} s).

The entanglement between the field and atomic states is analogous to the correlated two-particle states in the Einstein-Podolski-Rosen (EPR) paradox [14,20,21]. The two atomic states e and g are here correlated to the two field states $|-\alpha\rangle$ and $|\alpha\rangle$, respectively. Let us assume first that the cavity R_2 is left inactive. The atom crosses it and is detected downstream in two ionization zones D_e and D_g (see Fig. 1). Electric fields are applied to the atoms in these zones, producing atomic ionization. The resulting electrons are detected. The electric field in D_e is smaller than in D_g so that it ionizes the atoms in the e state, but not in the g state. The second zone D_g ionizes the atoms which remain in state g (see Fig. 1). This measurement projects the field in C either in the $|\alpha\rangle$ state (if the atom is detected in state g), or in the $|-\alpha\rangle$ state (if the atom is detected in state e).

However, as in an EPR experiment [21], one may choose to make another kind of measurement, by submitting the atom to a second $\pi/2$ pulse in R_2 . This pulse transforms again $|e\rangle$ into the state defined by Eq. (2.1) and $|g\rangle$ into $(-|e\rangle + |g\rangle)/\sqrt{2}$. The state (2.2) then gets transformed into

$$|\psi'_{\text{atom+field}}\rangle = \frac{1}{2}(|e; -\alpha\rangle - |e; \alpha\rangle + |g; \alpha\rangle + |g; -\alpha\rangle). \quad (2.3)$$

If one detects now the atom in the state $|g\rangle$ or $|e\rangle$, the field is projected into the state

$$|\psi_{\text{cat}}\rangle = \frac{1}{N_1}(|\alpha\rangle + e^{i\psi_1}|-\alpha\rangle), \quad (2.4)$$

where $N_1 = \sqrt{2[1 + \cos\psi_1 \exp(-2\alpha^2)]}$ and $\psi_1 = 0$ or π , according to whether the detected state is g or e , respectively. One produces therefore a coherent superposition of two coherent states, with phases differing by π . For $|\alpha|^2 \gg 1$, this is a ‘‘Schrödinger cat’’ state. The corresponding density operator is

$$\rho_F = \frac{1}{N_1^2}(|\alpha\rangle\langle\alpha| + |-\alpha\rangle\langle-\alpha| + e^{i\psi_1}|-\alpha\rangle\langle\alpha| + e^{-i\psi_1}|\alpha\rangle\langle-\alpha|). \quad (2.5)$$

We show below that by sending a second atom through the same system, it is possible to distinguish this state from the corresponding statistical mixture

$$\rho_F^{\text{mixture}} = \frac{1}{2}(|\alpha\rangle\langle\alpha| + |-\alpha\rangle\langle-\alpha|). \quad (2.6)$$

Note that for $|\alpha|^2 \gg 1$, (2.6) can be obtained from (2.5) by randomization of the phase ψ_1 .

Let us calculate now the probability of detecting the second atom in state $|e\rangle$ or $|g\rangle$, after it crosses the system $R_1 + C + R_2$. We neglect at this stage all relaxation effects. The state of the ‘‘second atom plus cavity field,’’ as the second atom leaves the first microwave zone R_1 , is now

$$|\psi_{\text{atom2+field}}^{(0)}\rangle = \frac{1}{\sqrt{2}}(|e_2\rangle + |g_2\rangle) \otimes \frac{1}{\sqrt{2}}(|\alpha\rangle + e^{i\psi_1}|-\alpha\rangle), \quad (2.7)$$

where we have assumed for simplicity that $|\alpha|^2 \gg 1$, so that the normalization factor in (2.4) becomes $1/\sqrt{2}$.

Right after the second atom leaves the superconducting cavity, and before it interacts with R_2 , the state of the system has evolved into

$$|\psi_{\text{atom2+field}}^{(1)}\rangle = \frac{1}{2}[|e_2; -\alpha\rangle + |g_2; \alpha\rangle + e^{i\psi_1}(|e_2; \alpha\rangle + |g_2; -\alpha\rangle)], \quad (2.8)$$

since the second atom dephases, as the first one, the field by an angle π if it is in state $|e\rangle$, and does not dephase the field at all, if its state is $|g\rangle$. Finally, after interacting with R_2 , the state of the system becomes

$$\begin{aligned} |\psi_{\text{atom2+field}}^{(2)}\rangle = & \frac{1}{2\sqrt{2}}[|e_2; -\alpha\rangle + |g_2; -\alpha\rangle + |g_2; \alpha\rangle \\ & - |e_2; \alpha\rangle + e^{i\psi_1}(|e_2; \alpha\rangle + |g_2; \alpha\rangle \\ & + |g_2; -\alpha\rangle - |e_2; -\alpha\rangle)]. \end{aligned} \quad (2.9)$$

Assuming again that $|\alpha\rangle$ and $|-\alpha\rangle$ are practically orthogonal, we get from (2.9) the probabilities for detecting the second atom in level g or e :

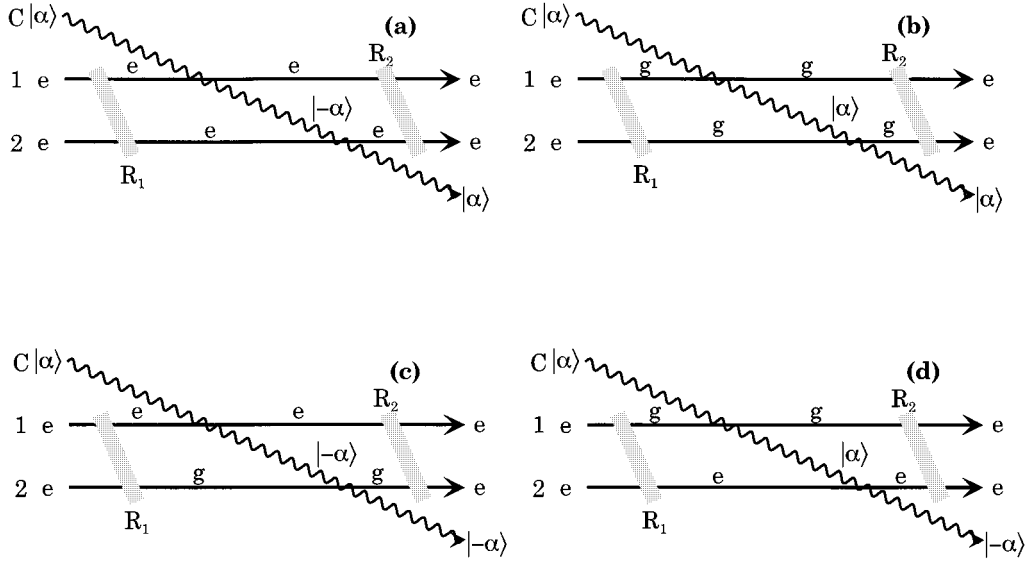


FIG. 2. Possible paths leading from a combined initial state $e-e$ of the two-atom system to final state $e-e$. In each diagram, the upper and lower lines are associated to the first and second atoms, respectively. The wiggled line is associated to the cavity state.

$$P(g_2) = \frac{1}{2}(1 + \cos\psi_1), \quad P(e_2) = \frac{1}{2}(1 - \cos\psi_1). \quad (2.10)$$

Since $\psi_1 = 0$ if the first atom was detected in state g , and $\psi_1 = \pi$ if the first atom was detected in state e , it follows from (2.10) that the second atom is always detected in the same state as the first one. There is thus a complete correlation between the two atoms.

The dependence on ψ_1 of the probabilities in (2.10) clearly displays the interference nature of the process. If there were a statistical mixture in C before atom 2 interacts with it, $P(g_2)$ and $P(e_2)$ would be equal to $1/2$ [randomization of ψ_1 in Eq. (2.10)].

The origin of the interference terms can be understood by interpreting the two-atom correlation measurement as a collision event between the two successive atoms, mediated by the system $R_1 + C + R_2$. A pair of atoms initially in level e is detected, after crossing the system, in a combined state $e-e$, $e-g$, $g-e$, or $g-g$, with the field in the cavity being left in either state $|\alpha\rangle$ or $|\alpha\rangle$. Each possible outcome may occur via two possible paths. For instance, the final state $e-e$ with the field in state $|\alpha\rangle$ may be obtained in two different ways: (i) both atoms cross the cavity in state e , remaining in this state after R_2 , so that the phase shift produced by the first atom is undone by the second; (ii) both atoms cross the cavity in state g , leaving the field unchanged, and flipping back to e in R_2 . These two paths, corresponding to diagrams (a) and (b) in Fig. 2, are totally indistinguishable and their amplitudes must thus interfere in the expression of the probability for the outcome $e-e$. Figure 2 also displays the paths (c) and (d) corresponding to the final state $|\alpha\rangle$ for the field. They do not interfere with the contributions from (a) and (b) as long as $|\alpha| \gg 1$. Note, however, that for $|\alpha| \leq 1$ all four contributions in Fig. 2 interfere with each other, due to the nonorthogonality of the coherent states $|\alpha\rangle$ and $|\alpha\rangle$.

B. Effect of dissipation: Exact solution

We consider now the effect of dissipation on the superposition of the two coherent states, and show that the decoherence can be monitored through the two-atom correlation measurement described above. Dissipation is described as a linear coupling of the field mode with a bath of thermal oscillators at zero temperature [22].

In order to describe dissipation, it is convenient to turn to a density-matrix formulation of the problem. We calculate $\rho_F(t)$, starting with $\rho_F(0)$ given by (2.5) using a method based on the calculation of the normal-ordered characteristic function corresponding to the field density operator [23]:

$$C_N(\lambda, \lambda^*, t) = \text{Tr} [\rho_F(t) e^{\lambda a^\dagger} e^{-\lambda^* a}]. \quad (2.11)$$

At time $t=0$, we have

$$C_N(\lambda, \lambda^*, 0) = \frac{1}{N_1^2} \{ e^{\lambda \alpha^* - \lambda^* \alpha} + e^{-\lambda \alpha^* + \lambda^* \alpha} + e^{-2|\alpha|^2} [e^{i\psi_1} e^{\lambda \alpha^* + \lambda^* \alpha} + e^{-i\psi_1} e^{-(\lambda \alpha^* + \lambda^* \alpha)}] \}. \quad (2.12)$$

The interaction with reservoir leads to the time development [13,23]

$$C_N(\lambda, \lambda^*, t) = C_N(\lambda e^{-\gamma t/2}, \lambda^* e^{-\gamma t/2}, 0), \quad (2.13)$$

where $\gamma = 1/t_c$ is the damping rate for the field intensity in the cavity, t_c being the corresponding damping time. In realistic experimental conditions [13,15], $t_c \approx 10^{-2}$ s. Therefore

$$C_N(\lambda, \lambda^*, t) = \frac{1}{N_1^2} \{ e^{(\lambda \alpha^* - \lambda^* \alpha) e^{-\gamma t/2}} + e^{(-\lambda \alpha^* + \lambda^* \alpha) e^{-\gamma t/2}} + e^{-2|\alpha|^2} [e^{i\psi_1} e^{(\lambda \alpha^* + \lambda^* \alpha) e^{-\gamma t/2}} + e^{-i\psi_1} e^{(-\lambda \alpha^* + \lambda^* \alpha) e^{-\gamma t/2}}] \}. \quad (2.14)$$

Comparing (2.11) and (2.14), we see that the density operator at time t is

$$\rho_F(t) = \frac{1}{N_1^2} [|\alpha e^{-\gamma t/2}\rangle \langle \alpha e^{-\gamma t/2}| + |-\alpha e^{-\gamma t/2}\rangle \langle -\alpha e^{-\gamma t/2}| + e^{-2|\alpha|^2(1-e^{-\gamma t})} (e^{i\psi_1} |-\alpha e^{-\gamma t/2}\rangle \langle \alpha e^{-\gamma t/2}| + e^{-i\psi_1} |\alpha e^{-\gamma t/2}\rangle \langle -\alpha e^{-\gamma t/2}|)]. \quad (2.15)$$

This equation displays the evolution of the system, from the pure state (2.4) to the mixture (2.6). For $t=0$, we recover the expression (2.5). The transition from (2.5) to (2.6) is governed by the exponential factor $\exp[-2|\alpha|^2(1-e^{-\gamma t})]$. For $\gamma t \ll 1$, this factor becomes $\exp(-2|\alpha|^2 \gamma t)$, implying that the coherent contribution to (2.15) decays with a lifetime equal to $t_c/2|\alpha|^2$. Thus the larger the average number of photons inside the cavity, the faster will the coherence decay. The decoherence time is shorter than the energy dissipation time in the cavity by a factor precisely equal to the ‘‘size’’ of the field measured by its photon number $|\alpha|^2$. For large fields ($2|\alpha|^2$ macroscopic), the decoherence time becomes of course exceedingly short [5]. This can be related to the basic mechanism by which coherence between the two positions of a pointer in a classical measurement apparatus disappears. In fact, the two fields $|\alpha\rangle$ and $|\alpha\rangle$ can be considered, when $|\alpha|^2 \gg 1$, as macroscopic pointers, related to the microscopic atomic state — the field will be left in state $|\alpha\rangle$ if the atom crosses the cavity in state $|g\rangle$, or in state $|\alpha\rangle$ if the atom is in state $|e\rangle$. We show now that the decoherence between these two field states can be monitored by sending another atom through the system.

C. Monitoring the decoherence

We assume that a second atom is sent through the cavity a time T after the first one. We assume that the time of flight of the atom through the system is very short compared to T and to the shortest time scale involved in the field relaxation (which, as shown in the preceding subsection, is of the order of $t_c/2|\alpha|^2$). The atom 2 plus field density operator just before the second atom goes into the superconducting cavity is given by

$$\rho_{\text{atom+field}}(T) = \frac{1}{2} (|e\rangle + |g\rangle) (\langle e| + \langle g|) \otimes \rho_F(T). \quad (2.16)$$

After the second atom goes through the cavity, we have

$$\rho_{\text{atom+field}} = \frac{1}{2} [|e\rangle \langle e| e^{-i\pi a^\dagger a} \rho_F(T) e^{i\pi a^\dagger a} + |g\rangle \langle g| \rho_F(T) + |e\rangle \langle g| e^{-i\pi a^\dagger a} \rho_F(T) + |g\rangle \langle e| \rho_F(T) e^{i\pi a^\dagger a}], \quad (2.17)$$

since the state $|e\rangle$ is always associated with a phase-shift operator $\exp(-i\pi a^\dagger a)$.

After the second atom interacts with the classical field in R_2 , the state of the system becomes

$$\rho_{\text{atom+field}} = \frac{1}{4} [(|e\rangle + |g\rangle) (\langle e| + \langle g|) e^{-i\pi a^\dagger a} \rho_F(T) e^{i\pi a^\dagger a} + (-|e\rangle + |g\rangle) (-\langle e| + \langle g|) \rho_F(T) + (|e\rangle + |g\rangle) (-\langle e| + \langle g|) e^{-i\pi a^\dagger a} \rho_F(T) + (-|e\rangle + |g\rangle) (\langle e| + \langle g|) \rho_F(T) e^{i\pi a^\dagger a}]. \quad (2.18)$$

From this expression, the probability of detecting the second atom in the e or g state is readily obtained:

$$P_{(g)}(T) = \frac{1}{2} (1 \pm \text{Re}\{\text{Tr}[e^{-i\pi a^\dagger a} \rho_F(T)]\}). \quad (2.19)$$

Replacing now in this expression $\rho_F(T)$ by (2.15), and using that

$$\begin{aligned} \text{Tr}[e^{-i\pi a^\dagger a} \rho_F(T)] &= \frac{1}{N_1^2} [\langle \alpha e^{-\gamma T/2} | -\alpha e^{-\gamma T/2} \rangle + \langle -\alpha e^{-\gamma T/2} | \alpha e^{-\gamma T/2} \rangle \\ &\quad + e^{-2|\alpha|^2(1-e^{-\gamma T})} (e^{i\psi_1} \langle \alpha e^{-\gamma T/2} | \alpha e^{-\gamma T/2} \rangle + e^{-i\psi_1} \langle -\alpha e^{-\gamma T/2} | -\alpha e^{-\gamma T/2} \rangle)] \\ &= \frac{2}{N_1^2} [e^{-2|\alpha|^2 e^{-\gamma T}} + e^{-2|\alpha|^2(1-e^{-\gamma T})} \cos\psi_1], \end{aligned} \quad (2.20)$$

we get, finally,

$$P_{(g)}(T) = \frac{1}{2} \left[1 \pm \frac{e^{-2|\alpha|^2 e^{-\gamma T}} + \cos\psi_1 e^{-2|\alpha|^2(1-e^{-\gamma T})}}{1 + \cos\psi_1 e^{-2|\alpha|^2}} \right]. \quad (2.21)$$

For $|\alpha| \gg 1$, and $T=0$, we recover the results for the corresponding dissipationless case [cf. Eq. (2.10)]. If now $t_c \gg T \gg t_c/2|\alpha|^2$, again with $|\alpha| \gg 1$, we get from (2.21) that

the detection probability is 1/2, which is the classical statistics result. In this time interval the interference term in (2.15) goes to zero, and $\rho_F(T)$ turns into a statistical mixture. When T increases so that $\gamma T \gg 1$, one gets again $P_g=1$ and $P_e=0$. In this limit, the two states $|\alpha\rangle$ and $|\alpha\rangle$ relax towards the vacuum, and are not orthogonal anymore. As soon as they start to overlap, interference effects, associated with the evolution of the atomic coherence between the two microwave zones, become important. In terms of the diagrams

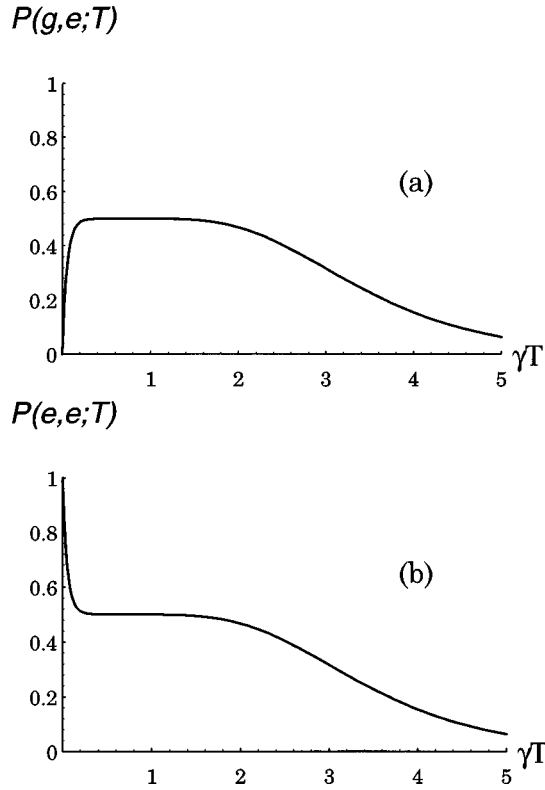


FIG. 3. (a) Conditional probability $P(g, e; T)$ of detecting the second atom in level e after having detected the first one in level g , as a function of the delay T between the two atoms, for the experiment sketched in Fig. 1. The average number of photons in the cavity is equal to 10. (b) Conditional probability $P(e, e; T)$.

displayed in Fig. 2, this means that paths (c) and (d) now start interfering with (a) and (b). In particular, when the field has finally relaxed to the vacuum, the cavity no longer has any effect on the atoms and the combined effects of the two $\pi/2$ pulses amounts to a π pulse. Thus, and independently of the state in which the first atom was detected, the second atom should come out in a state different from the state in which it has come in (i.e., in state g). The plot of the conditional probabilities $P(g, e; T) \equiv P_e(T, \psi_1 = 0)$ and $P(e, e; T) \equiv P_e(T, \psi_1 = \pi)$ for detecting the second atom in level e after having detected the first one, respectively, in levels g and e , as a function of the delay T between the two atoms, is shown in Fig. 3 (for an initial state with average number of photons $\bar{n} = 10$). The fast evolution around $T = 0$ reveals the rapid decoherence process between the two orthogonal components of the mesoscopic field. The plateaus $P(g, e; T) = P(e, e; T) = 1/2$ are the signature of a classical mixture involving two orthogonal field states in the cavity. The slow decay at large times indicates that the two states of the incoherent superposition start to overlap due to field energy dissipation.

D. Effect of velocity dispersion

The experiment proposed above must be performed with quasimonokinetic beams ensuring well-defined interaction times with the R_1 , C , and R_2 cavities. Let us estimate now the effect of a small velocity mismatch between the two at-

oms. We assume a simple model where the first atom has the velocity corresponding to an exact π phase shift for the field in C when the atom crosses the cavity in e , and where the second atom has a slightly different velocity.

The second atom velocity mismatch has two consequences. First, it produces for this atom a departure from the ideal pulse area in R_1 and R_2 . Second, the phase shift of the coherent state in the superconducting cavity when this atom crosses it in e becomes $\pi + \epsilon$ with $|\epsilon| \ll 1$. While the first effect alters the coefficients in the superpositions (2.16) and (2.18), the second affects the phases of the interfering contributions. For a qualitative analysis, we take only this second effect into consideration here, since it is by far the most important one. The probabilities of finding the atom in the states e and g after it crosses the system become now

$$P_{(g)}(T) = \frac{1}{N_1} (1 \pm \text{Re}\{\text{Tr}[e^{-i(\pi+\epsilon)a^\dagger a} \rho_F(T)]\}). \quad (2.22)$$

If we take for $\rho_F(T)$ the result (2.15), we get

$$P_{(g)}(T) = \frac{1}{2} \left\{ 1 \pm \frac{\cos(|\alpha|^2 e^{-\gamma T} \sin \epsilon)}{1 + \cos \psi_1 e^{-2|\alpha|^2}} [e^{-2|\alpha|^2} e^{-\gamma T \cos^2(\epsilon/2)} + \cos \psi_1 e^{-2|\alpha|^2 [1 - e^{-\gamma T \cos^2(\epsilon/2)}]}] \right\}, \quad (2.23)$$

which, for $\epsilon \ll 1$, becomes

$$P_{(g)}(T) \approx \frac{1}{2} \left\{ 1 \pm \frac{\cos(|\alpha|^2 e^{-\gamma T} \epsilon)}{1 + \cos \psi_1 e^{-2|\alpha|^2}} [e^{-2|\alpha|^2} e^{-\gamma T} + \cos \psi_1 e^{-2|\alpha|^2 (1 - e^{-\gamma T})}] \right\}. \quad (2.24)$$

The conditional probability corresponds to the average of this expression over the allowed range of values for ϵ . Comparison of (2.24) with (2.21) displays the loss of contrast as the dispersion in the values of ϵ increases. The velocity dispersion of the atomic beam makes the probability approach the incoherent value $1/2$ as the range of values of ϵ increases. The departure of the probability from the value $1/2$ at short times T can, however, be observed up to $|\alpha|^2 \epsilon$ of the order of unity. This is displayed in Fig. 4 where we show $P(g, e; T)$. For $|\alpha|^2 = 100$, the observation of quantum coherence requires $\epsilon \ll 10^{-2}$, which corresponds to a velocity dispersion of about 1%, easily achievable with today's laser cooling techniques.

E. Effect of unread atoms

Let us discuss now the effect of a finite detection efficiency. More precisely, let us assume that an undetected atom has crossed the cavity between the atom which prepares the mesoscopic field and the probe atom. After the undetected atom, the field density operator becomes

$$\rho_F^{\text{unread}} = \text{Tr}_{\text{atom}}[\rho_{\text{atom} + \text{field}}], \quad (2.25)$$

where $\rho_{\text{atom} + \text{field}}$ can be taken as (2.17) or (2.18)—the existence of the second microwave region R_2 is not relevant for

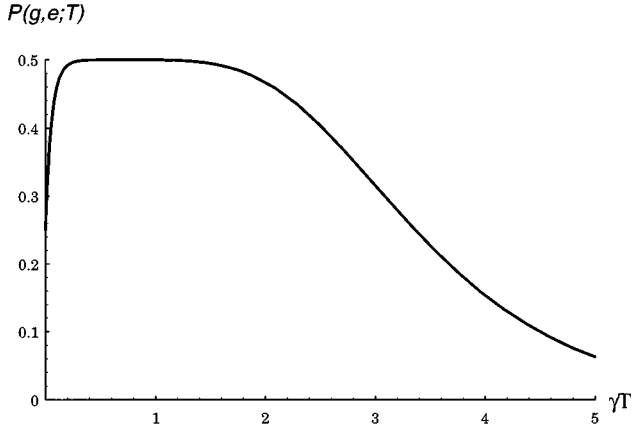


FIG. 4. Effect of velocity dispersion on the conditional probability $P(g, e; T)$ shown in Fig. 3(a). We take here $|\alpha|^2 \epsilon = \pi/3$. The average number of photons $|\alpha|^2$ is 10.

this atom, which is not measured. One gets then in the general case where the phase shift produced by the second atom is given by ϕ

$$\rho_F^{\text{unread}} = \frac{1}{2}(e^{-i\phi a^\dagger a} \rho_F e^{i\phi a^\dagger a} + \rho_F). \quad (2.26)$$

Using the invariance of the trace by circular permutation, it is easy to see that the replacement of $\rho_F(T)$ in (2.22) by ρ_F^{unread} does not change the detection probabilities for the probe atom.

Therefore a high detection efficiency is not required to monitor the decoherence process. Of course, it is still necessary to make the two successive detections in a time smaller than the decoherence time $t_c/2|\alpha|^2$. For a cavity damping time equal to 10^{-2} s, an average number of photons in the cavity of the order of 100, and an atomic flux of 10^5 atoms per second, it is sufficient to detect about one in every ten atoms in order to display the coherence between the two dephased field states.

III. OPTICAL SWITCH WITH QUANTUM COHERENCE BETWEEN “OPEN” AND “CLOSED” STATES

A. Preparation of the switch

In [15] a method was proposed for preparing an optical “quantum switch,” in a superposition of “open” and “closed” states. The experimental setup is the same as above (see Fig 1). A single atom prepared in a superposition of different energy states is sent across the high- Q cavity C (resonance frequency ω_c) coupled to the monochromatic classical radiation source S (frequency ω_s). The source is now nonresonant, with a detuning $\Delta = \omega_s - \omega_c$ much larger than the cavity bandwidth $\omega_c/Q = 1/t_c$, so that no photons are fed into the empty cavity. The situation may change, however, as the atom crosses the cavity. As in Sec. II, we assume that state e is closer to resonance than state g , being coupled to a third, more excited, state $|i\rangle$ by a transition at frequency $\omega_0 = \omega_c - \delta$ (Fig. 5). The coupling of the $e \rightarrow i$ transition to the cavity mode is characterized by the vacuum Rabi frequency Ω . As before, we assume that the geometry of the mode and the atomic velocity are such that the coupling is adiabatically switched on and off, as the atom enters

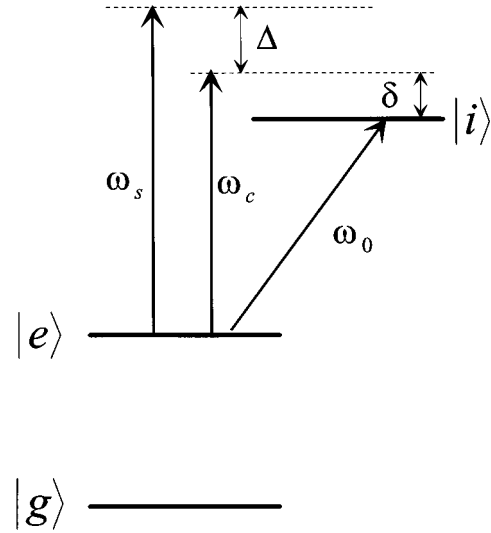


FIG. 5. Sketch of the atomic levels relevant to the quantum switch experiment.

and exits the cavity. Provided the field amplitude remains small enough, an atom in level e pulls the mode frequency by Ω^2/δ . If the detunings are adjusted so that $\Delta = \Omega^2/\delta$, the atom in level e tunes the cavity into resonance with the source, while no frequency pulling occurs if the atom crosses the cavity in level g . Due to the adiabatic nature of the coupling, the atom remains in the same state while crossing the cavity.

Assume now, as above, that an atom is prepared in the state (2.1), through the first Ramsey region R_1 . A subsequent detection in the state $|e\rangle$ or $|g\rangle$, after the atom has undergone another $\pi/2$ pulse in R_2 , leaves the field in the state

$$|\psi_F\rangle = \frac{1}{N_2}(|\alpha\rangle + e^{i\psi_1}|0\rangle), \quad (3.1)$$

where again $\psi_1 = 0$ or π according to whether the atom is detected in state $|g\rangle$ or $|e\rangle$, respectively, and N_2 is the normalization constant $N_2 = \{2[1 + \cos\psi_1 \exp(-|\alpha|^2)]\}^{1/2}$, which reduces to $\sqrt{2}$ when $|\alpha|^2 \gg 1$. The state (3.1) is a quantum superposition of cavity “filled” and “empty” states. For $|\alpha| \gg 1$, it is a Schrödinger cat state.

B. Measuring the coherence by detection of a second atom

We show now that a two-atom correlation measurement allows us again to distinguish the state (3.1) from a statistical mixture. A second probe atom is sent through the system a time T after the first atom comes into the cavity, and the probability that this atom is in state e or g is measured. We neglect at this stage field dissipation. The second atom is also prepared in the state (2.1), so that, just before it enters C , the state of the combined system atom 2 plus field can be written as

$$|\psi_{\text{atom2+field}}\rangle = \frac{1}{N_2\sqrt{2}}(|e\rangle + |g\rangle) \otimes (|\alpha\rangle + e^{i\psi_1}|0\rangle). \quad (3.2)$$

The second atom will have an effect on the field in the cavity only if it is in state $|e\rangle$. In this case, it will add the

field $\alpha e^{-i\Delta T}$ into the cavity, and at the same time will dephase an already present field by Δt_i , where t_i is the interaction time between the atom and the cavity field. Therefore after the second atom crosses the cavity there are four possibilities for the state of the field: either the cavity ends up empty or containing one of the three fields α , $\alpha e^{-i\Delta T}$, or $\alpha(e^{-i\Delta T} + e^{-i\Delta t_i})$. The effect of the second atom on the field can be expressed in terms of a phase-shift operator $e^{-i\Delta t_i a^\dagger a}$ and a displacement operator $D(\alpha e^{-i\Delta T})$, defined by [16]

$$D(\alpha) = e^{\alpha a^\dagger - \alpha^* a}. \quad (3.3)$$

After the second atom exits the cavity, the state of the system becomes

$$|\psi_{\text{atom2+field}}\rangle = \frac{1}{\sqrt{2}}[|e\rangle(\mathcal{S}|\psi_F\rangle) + |g\rangle|\psi_F\rangle], \quad (3.4)$$

where $|\psi_F\rangle$ is given by (3.1), and we have defined

$$\mathcal{S} = D(\alpha e^{-i\Delta T})e^{-i\Delta t_i a^\dagger a}. \quad (3.5)$$

After the second atom goes through the region R_2 , the state of the system becomes

$$|\psi_{\text{atom2+field}}\rangle = \frac{1}{2}[|e\rangle(\mathcal{S}-1)|\psi_F\rangle + |g\rangle(\mathcal{S}+1)|\psi_F\rangle]. \quad (3.6)$$

The probability of detecting the second atom in the state e or g can be obtained by calculating the trace of the density operator corresponding to state (3.6) multiplied by the projectors $|e\rangle\langle e|$ or $|g\rangle\langle g|$, respectively:

$$P_{(g)} = \frac{1}{2}\{1 \pm \text{Re}[\text{Tr}(\mathcal{S}|\psi_F\rangle\langle\psi_F|)]\}. \quad (3.7)$$

We calculate now explicitly this expression, for the state $|\psi_F\rangle$ given by (3.1). We use that, for a coherent state $|\alpha\rangle$,

$$\mathcal{S}|\alpha\rangle = e^{i\phi_\alpha}|\alpha(e^{-i\Delta T} + e^{-i\Delta t_i})\rangle, \quad (3.8)$$

where

$$\phi_\alpha = |\alpha|^2 \sin[\Delta(t_i - T)]. \quad (3.9)$$

Also,

$$\mathcal{S}|0\rangle = |\alpha e^{-i\Delta T}\rangle. \quad (3.10)$$

We get then

$$P_{(g)} = \frac{1}{2} \left\{ 1 \pm \frac{1}{2(1 + \cos\psi_1 e^{-|\alpha|^2/2})} \text{Re}[\langle 0|\alpha e^{-i\Delta T}\rangle + e^{i\phi_\alpha} \langle \alpha|\alpha(e^{-i\Delta T} + e^{-i\Delta t_i})\rangle + e^{i\phi_\alpha} \langle \alpha e^{-i\psi_1}|\alpha(e^{-i\Delta T} + e^{-i\Delta t_i})\rangle + e^{i\psi_1} \langle \alpha|\alpha e^{-i\Delta T}\rangle] \right\}. \quad (3.11)$$

In this expression, each scalar product measures the overlap of two possible field states in the cavity. As in the discussion of Sec. II, an important overlap means that an interference process involving indistinguishable final field states can take

place. When $|\alpha|^2 \gg 1$, the first scalar product in Eq. (3.11) is negligible. The second one is also negligible, except when simultaneously $\Delta T \approx \pm \pi/3$ (modulo 2π) and $\Delta t_i \approx \mp \pi/3$ (modulo 2π). The corresponding interference is thus accidental (it requires a specific velocity for the atom), and will be disregarded in the following. Keeping only the last two interference terms, we get then, for $|\alpha|^2 \gg 1$,

$$P_{(g)} = \frac{1}{2} \left(1 \pm \frac{1}{2} \{ e^{-2|\alpha|^2 \cos^2[\Delta(T-t_i)/2]} \cos(\phi_\alpha - \psi_1) + e^{-2|\alpha|^2 \sin^2(\Delta T/2)} \cos[\psi_1 - |\alpha|^2 \sin(\Delta T)] \} \right). \quad (3.12)$$

The dependence on ψ_1 of the terms between curly braces is a signature of their interference character. For random ψ_1 , we get the result for a statistical mixture (i.e., $P_{(g)} = 1/2$), as expected.

On the other hand, for fixed ψ_1 , we see that $P_{(g)}$ presents peaks or dips when $\Delta(T-t_i)/\pi$ is an odd integer or $\Delta T/\pi$ is an even one, and is equal to a $1/2$ ‘‘background’’ for other values of T and t_i [15]. The width of these peaks is of the order of $1/|\alpha|$. The values of $P_{(g)}$ for these values of T and t_i are

$$P_{(g)} = \frac{1}{2} (1 \pm \frac{1}{2} \cos\psi_1), \quad (3.13)$$

so that, if $P(a_1, a_2)$ is the conditional probability that the first and second atom are measured in states a_1 and a_2 , respectively, we have

$$P(g, g) = P(e, e) = \frac{3}{4}, \quad P(e, g) = P(g, e) = \frac{1}{4}. \quad (3.14)$$

For $\Delta t_i = (2k+1)\pi$, $k=0,1,2,\dots$, the two sets of peaks merge, and we get instead

$$P_{(g)} = \frac{1}{2} (1 \pm \cos\psi_1), \quad (3.15)$$

so that now the contrast is increased and the peak values of $P(a_1, a_2)$ become

$$P(g, g) = P(e, e) = 1, \quad P(e, g) = P(g, e) = 0. \quad (3.16)$$

Figure 6 displays the conditional probability $P(g, g; T) = P(e, e; T)$ as a function of the delay between the two atoms, for $|\alpha|^2 = 10$ and $\Delta t_i = 7\pi/2$. The interference peaks are superimposed to a $\frac{1}{2}$ ‘‘background.’’

Experimentally, these curves could be obtained by measuring the corresponding conditional probabilities over a large number of double atom counts, in such a way that the first atom is always sent in an empty cavity system (obtained by waiting long enough for the field in the cavity to relax to the vacuum). Since the atomic distribution in the beam is Poissonian, the time delay T will necessarily vary (the range of variation can be controlled by changing the atomic flux). For each run, it can be determined by timing the successive detections of atoms 1 and 2. Of course, the first peaks in Fig. 6 are not observable, since T must be larger than the time of flight of the first atom through the cavity C .

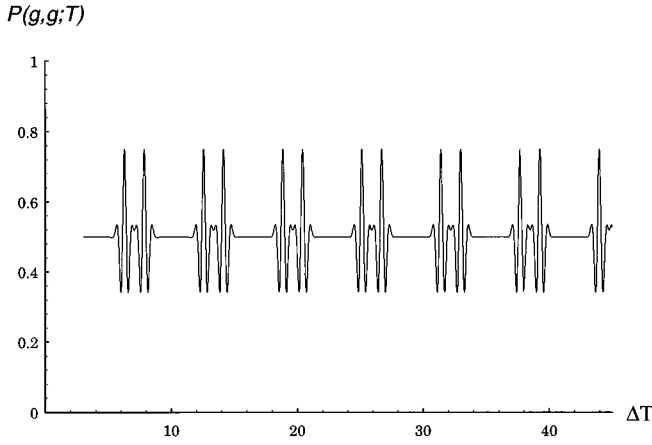


FIG. 6. Probability $P(g,g;T)$ to detect in the quantum switch experiment the first and the second atom in the same state g as a function of the delay T between the two atoms ($|\alpha|^2=10, \Delta t_i=7\pi/2$). Cavity relaxation is neglected.

C. Monitoring the decoherence due to dissipation

As in Sec. II, dissipation will again cause coherence to disappear in a time which gets smaller as the intensity of the field grows. Between the production of the state, through detection of the first atom, and the detection of the probe atom, the state of the field evolves towards a statistical mixture. The probability of detecting the second atom in state g or e is now

$$P_{(g)}(T) = \frac{1}{2}(1 \pm \text{Re}\{\text{Tr}[\mathcal{T}\rho_F(T)]\}), \quad (3.17)$$

where $\rho_F(T)$ is the reduced density matrix of the field in the cavity, at the time T when it is crossed by the second atom (we assume again $t_i \ll t_c/|\alpha|^2$).

The calculation of $\rho_F(T)$ follows closely the method used in Sec. II, and is done in Appendix A. In the limit $|\alpha|^2 \gg 1$, we get

$$\begin{aligned} P_{(g)}(T) &= \frac{1}{2}\{1 \pm \frac{1}{2}e^{|\alpha|^2(e^{-\gamma T/2}\cos\Delta T - 1)} \\ &\quad \times \cos(\psi_1 - |\alpha|^2e^{-\gamma T/2}\sin\Delta T) \\ &\quad \pm \frac{1}{2}e^{-|\alpha|^2[e^{-\gamma T/2}\cos\Delta(T-t_i) + 1]} \\ &\quad \times \cos[\psi_1 + |\alpha|^2e^{-\gamma T/2}\sin\Delta(T-t_i)]\}. \end{aligned} \quad (3.18)$$

As before, we get peaks or dips when $\Delta T/\pi$ is an even integer or $\Delta(T-t_i)/\pi$ is an odd one. In this case, we get

$$P_{(g)}(T) = \frac{1}{2}[1 \pm \frac{1}{2}\cos\psi_1 e^{|\alpha|^2(e^{-\gamma T/2} - 1)}]. \quad (3.19)$$

Moreover, if Δt_i is an odd integer, then

$$P_{(g)}(T) = \frac{1}{2}[1 \pm \cos\psi_1 e^{|\alpha|^2(e^{-\gamma T/2} - 1)}]. \quad (3.20)$$

These equations coincide with those obtained in the dissipationless case when $T=0$. On the other hand, when $|\gamma|T \ll 1$, (3.19) and (3.20) become, respectively,

$$P_{(g)}(T) = \frac{1}{2}(1 \pm \frac{1}{2}\cos\psi_1 e^{-|\alpha|^2\gamma T/2}) \quad (3.21)$$

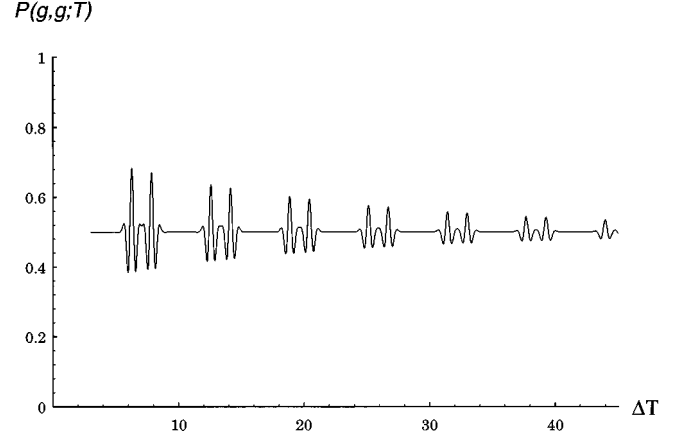


FIG. 7. $P(g,g;T)$ in the quantum switch experiment with cavity relaxation included ($1/t_c = \Delta/100$).

and

$$P_{(g)}(T) = \frac{1}{2}(1 \pm \cos\psi_1 e^{-|\alpha|^2\gamma T/2}). \quad (3.22)$$

These equations show that the interference term decreases with a lifetime $2t_c/|\alpha|^2$, which gets smaller as the average number of photons $|\alpha|^2$ increases (see Fig. 7). The quantity $t_c/|\alpha|^2$ sets up, here too, the time scale within which the pure state gets transformed into a statistical mixture. By sampling double atom counts within this time scale, one can thus monitor the decoherence between the two states of the field in the cavity. For $|\alpha|^2=10$, and $\gamma=1/t_c=100 \text{ s}^{-1}$, this implies an upper limit of the order of 1 ms for the time interval T between successive atoms, in order that the interference effect be seen. This interval is easily achievable with the Rydberg atom beams presently available (fluxes of the order of 10^5 atoms per second).

D. Effect of velocity dispersion

We consider here the effect of the dispersion in atomic velocities on the height of the interference peaks. We assume the first atom leaves the field in the state

$$|\psi_F\rangle = \frac{1}{\sqrt{2}}(|\alpha\rangle + e^{i\psi_1}|0\rangle), \quad (3.23)$$

where α depends of course on the atomic speed.

As in Sec. II, we consider here only the effect of velocity dispersion on the relative phases of the interfering contributions, neglecting the changes of the coefficients of the states due to the departure of the pulses in R_1 and R_2 from the ideal $\pi/2$ situation. Right after the second atom crosses the second Ramsey region, the state of the system atom 2 plus field is

$$|\psi\rangle = \frac{1}{2}[|e\rangle(\mathcal{T}' - 1) + |g\rangle(\mathcal{T}' + 1)]|\psi\rangle, \quad (3.24)$$

where now

$$\mathcal{T}' = D(\alpha' e^{-i\Delta T}) e^{-i\Delta t'_i a^\dagger a}, \quad (3.25)$$

with

$$\alpha' = k\alpha, \quad k \text{ real} \quad (3.26)$$

while t'_i is the interaction time between atom 2 and the superconducting cavity. These expressions take into account the fact that the different atomic velocity implies a change in the interaction time, and consequently different values for the phase shift of the field already present in the cavity, as well as for the amplitude of the field injected in the cavity due to the presence of the second atom.

As before, the probability of finding the second atom in state $|e\rangle$ or $|g\rangle$ is

$$P_{(g)} = \frac{1}{2} \{1 \pm \text{Re}[\text{Tr}(\mathcal{F}' |\psi_F\rangle\langle\psi_F|)]\}, \quad (3.27)$$

where now

$$\mathcal{F}'|\alpha\rangle = e^{ik\phi'_\alpha} |\alpha(k e^{-i\Delta T} + e^{-i\Delta t'_i})\rangle \quad (3.28)$$

and

$$\phi'_\alpha = |\alpha|^2 \sin[\Delta(t'_i - T)]. \quad (3.29)$$

Also,

$$\mathcal{F}'|0\rangle = |k\alpha e^{-i\Delta T}\rangle. \quad (3.30)$$

We take for simplicity the situation of ‘‘merging peaks,’’ that is, $\Delta T/\pi$ equal to an even integer and $\Delta t_i/\pi$ equal to an odd one. The analysis is similar, and leads to the same conclusions, in the case in which the peaks do not merge. We also consider $|\alpha|^2 \gg 1$. Then,

$$\begin{aligned} \text{Tr}(\mathcal{F}' |\psi_F\rangle\langle\psi_F|) &= \frac{1}{2} [e^{-i\psi_1} \langle 0|\alpha(k-1)\rangle + \langle 0|k\alpha\rangle + e^{i\psi_1} \langle \alpha|k\alpha\rangle] \\ &= \frac{1}{2} [e^{-i\psi_1} e^{-|\alpha|^2(k-1)^2/2} + e^{-|\alpha|^2 k^2/2} + e^{i\psi_1} e^{-|\alpha|^2(k-1)^2/2}] \\ &\approx e^{-|\alpha|^2(k-1)^2/2} \cos\psi_1 \end{aligned} \quad (3.31)$$

and

$$P_{(g)} \approx \frac{1}{2} [1 \pm e^{-|\alpha|^2(k-1)^2/2} \cos\psi_1] \quad (|\alpha|^2 \gg 1). \quad (3.32)$$

Comparing this expression with (3.15), we see that the contrast decreases as $\exp[-|\alpha|^2(k-1)^2/2]$. The interference peaks remain detectable as long as $|\alpha|^2(k-1)^2 < 1$, that is, $|\alpha|^2(\Delta k)^2 < 1$, where Δk is related to the velocity dispersion by $\Delta k \approx \Delta k/k = \Delta t_i/t_i = \Delta v/v$. Therefore this condition implies that one should have $\Delta v/v < 1/|\alpha|$. For $|\alpha|^2 \approx 100$, this means that the velocity dispersion should be smaller than 10%.

Let us finally discuss briefly the effect of a finite detection efficiency. As opposed to the coherent superposition of fields with different phases considered in Sec. II, unread atoms must have here a strong effect, since they allow a random field to be injected in the cavity. This clearly washes out all interference effects.

IV. NONLOCAL MICROWAVE FIELDS

Nonlocal field states can be prepared by the combination of two quantum switches [15]. Figure 8 shows the experi-

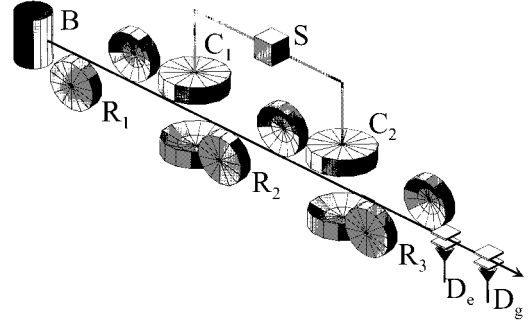


FIG. 8. Sketch of the nonlocal field experiment.

mental arrangement. Two identical high- Q cavities C_1 and C_2 are coupled to the same microwave source S . An atom crosses the apparatus and experiences $\pi/2$ pulses before C_1 and after C_2 , in the low- Q cavities R_1 and R_3 , while a π pulse is applied in R_2 , between C_1 and C_2 . This π pulse performs the transformation $|e\rangle \rightarrow |g\rangle$ and $|g\rangle \rightarrow -|e\rangle$. The two cavities are initially in the vacuum state, and S is detuned so that a field is injected in C_1, C_2 only if the atom crosses the cavity in state $|e\rangle$ (the atom interacts dispersively with the cavity field—see Fig. 5 for the level scheme).

Right after the atom goes through R_1 , the combined state of the system is given by

$$|\psi_1\rangle = \frac{1}{\sqrt{2}} (|e\rangle + |g\rangle) |0,0\rangle, \quad (4.1)$$

where $|0,0\rangle$ specifies that the fields in both cavities are in the vacuum state. After the atom goes through the first cavity, but before it crosses R_2 , we have

$$|\psi_2\rangle = \frac{1}{\sqrt{2}} (|e\rangle |\alpha,0\rangle + |g\rangle |0,0\rangle). \quad (4.2)$$

Right after the atom crosses R_2 , the state of the system will be

$$|\psi_3\rangle = \frac{1}{\sqrt{2}} (|g\rangle |\alpha,0\rangle - |e\rangle |0,0\rangle). \quad (4.3)$$

After the atom leaves the second cavity, we get

$$|\psi_4\rangle = \frac{1}{\sqrt{2}} (|g\rangle |\alpha,0\rangle - |e\rangle |0, \alpha e^{-i\phi_0}\rangle), \quad (4.4)$$

where $\phi_0 = \Delta t$ is the phase shift between the cavity mode and the source during the atom time of flight t between C_1 and C_2 . This phase can be compensated by the introduction of a dephaser between the source and the second cavity. We assume in the following that this compensation is performed, and write therefore, instead of $|\psi_4\rangle$,

$$|\psi'_4\rangle = \frac{1}{\sqrt{2}} (|g\rangle |\alpha,0\rangle - |e\rangle |0, \alpha\rangle). \quad (4.5)$$

Finally, after R_3 , the state of the system becomes

$$|\psi_5\rangle = \frac{1}{2} [(|\alpha,0\rangle - |0,\alpha\rangle) |g\rangle - (|\alpha,0\rangle + |0,\alpha\rangle) |e\rangle]. \quad (4.6)$$

After detection of the atom in state $|e\rangle$ or $|g\rangle$, the field is projected in the state

$$|\psi_f\rangle = \frac{1}{N_3} (|\alpha, 0\rangle + e^{i\psi_1}|0, \alpha\rangle), \quad (4.7)$$

where $\psi_1=0$ or π according to whether state $|e\rangle$ or $|g\rangle$ is detected, respectively, and $N_3 = [2(1 + \cos\psi_1 e^{-|\alpha|^2})]^{1/2}$.

Equation (4.7) represents a coherent superposition of two states, which describes a coherent field located either in the first or in the second cavity. The sharing of one photon between two cavities has been considered before [24], but the state considered here is quite different in nature. For $|\alpha|^2 \gg 1$, this nonlocal field is related at the same time to two paradoxes of quantum mechanics: while the superposition of two macroscopically distinguishable classical states of the field can be viewed as a Schrödinger cat, the nonlocal correlation of field states is typical of EPR experiments. Furthermore, state (4.7) is intimately connected to the measurement problem in quantum mechanics: the field in the double cavity can be considered as a classical pointer, whose position measures the internal microscopic state of the atom crossing the system. If the atom comes into the first cavity in the state $|e\rangle$, instead of the superposition state created by R_1 , it is easy to see that, after crossing the second cavity, the field is left in the state $|\alpha, 0\rangle$, while if the atom comes in the state $|g\rangle$ the field is left in the state $|0, \alpha\rangle$. Therefore the state of the double-cavity system can be used as a pointer, which measures the incoming microscopic atomic state. The two-cavity system can thus be considered as a macroscopic measuring apparatus (if $|\alpha|^2 \gg 1$), which interacts with a microscopic system (the two-level atom). When the atom comes into this ‘‘measuring apparatus’’ in a coherent superposition of the states $|e\rangle$ and $|g\rangle$, the system evolves into the entangled state given by (4.4). The transformation of this entangled state into a statistical mixture is an essential stage of the measurement process [3, 5–9]. As in the previous examples, this transformation is a decoherence process associated with the interaction between the two-cavity system and the external world, modeled here by a heat reservoir. We show in the following that it is possible to measure the coherence between the two positions of the pointer, and follow the process of decoherence in an actual experiment. The two-cavity system leads therefore not only to an exactly soluble model of the measurement process, simulating the spatially distinct positions of a classical pointer, and including the role of dissipation, but is also sufficiently realistic to foresee an experimental verification.

A. Detection of the state

The distinction between state (4.7) and the corresponding statistical mixture may again be demonstrated through a two-atom correlation experiment. A time T after preparation of the field state (4.7), a probe atom identical to the first one is sent through the system. At this stage, we assume that the two atoms have the same velocity and we neglect field relaxation.

The effect on the two cavities of the probe atom in state e is represented by the unitary operators

$$\mathcal{F}_l = D_l(\alpha e^{-i\Delta T}) e^{-i\Delta t_l a_l^\dagger a_l}, \quad l=1,2 \quad (4.8)$$

with

$$D_l(\alpha e^{-i\Delta T}) = e^{\alpha e^{-i\Delta T} a_l^\dagger - \alpha^* e^{i\Delta T} a_l}. \quad (4.9)$$

After the atom leaves R_3 , the state of the combined atom 2 plus cavities system is

$$|\psi_{\text{atom2} + \text{field}}\rangle = \frac{1}{2} [-|e\rangle(\mathcal{F}_1 + \mathcal{F}_2) + |g\rangle(\mathcal{F}_1 - \mathcal{F}_2)] |\psi_F\rangle. \quad (4.10)$$

The probabilities of detecting atom 2 in states $|e\rangle$ or $|g\rangle$ are, respectively,

$$P_{(g)} = \frac{1}{2} \{1 \pm \text{Re}[\text{Tr}(\mathcal{F}_1 |\psi_F\rangle \langle \psi_F| \mathcal{F}_2^\dagger)]\}. \quad (4.11)$$

Replacing (4.7) in (4.11), we get

$$P_{(g)} = \frac{1}{2} \left\{ 1 \pm \frac{1}{N_3^2} \text{Re}[\langle \alpha, \alpha e^{-i\Delta T} | \alpha(e^{-i\Delta T} + e^{-i\Delta t_i}), \alpha \rangle e^{i\phi_\alpha} \right. \\ \left. + \langle 0, \alpha(e^{-i\Delta T} + e^{-i\Delta t_i}) | \alpha e^{-i\Delta T}, \alpha \rangle e^{-i\phi_\alpha} \right. \\ \left. + \langle \alpha, \alpha e^{-i\Delta T} | \alpha e^{-i\Delta T}, \alpha \rangle e^{i\psi_1} \right. \\ \left. + \langle 0, \alpha(e^{-i\Delta T} + e^{-i\Delta t_i}) | \alpha(e^{-i\Delta T} + e^{-i\Delta t_i}), 0 \rangle e^{-i\psi_1} \right\}, \quad (4.12)$$

with ϕ_α given by (3.9). When $|\alpha|^2 \gg 1$, the first two terms in the expression between square brackets become negligible. We get then,

$$P_{(g)} \approx \frac{1}{2} \{1 \pm \frac{1}{2} \cos\psi_1 [e^{-2|\alpha|^2(1-\cos\Delta T)} \\ + e^{-2|\alpha|^2\{1+\cos[\Delta(t_i-T)]\}}]\}. \quad (4.13)$$

The term proportional to $\cos\psi_1$ is the interference contribution. For random ψ_1 , which corresponds to a statistical mixture, we get $P_{(g)} = 1/2$. For $\psi_1 = 0$ or π , we get peaks whenever $\Delta T/\pi$ is an even integer, or $\Delta(t_i - T)/\pi$ is an odd one. Then the conditional probability $P(a_1, a_2)$ is given again by (3.14). If, besides, $\Delta t_i/\pi$ is an odd integer, both series of peaks coincide, and $P(a_1, a_2)$ is given by (3.16).

B. Dissipation and decoherence

The evolution of the field density operator under the action of dissipation is calculated in the same way as in the previous two cases. The details are given in Appendix B. When $|\alpha|^2 \gg 1$, the conditional probability for detecting the probe atom in states $|e\rangle$ or $|g\rangle$ is now

$$P_{(g)}(T) \approx \frac{1}{2} \{1 \pm \frac{1}{2} \cos\psi_1 [e^{2|\alpha|^2(e^{-\gamma T/2} \cos\Delta T - 1)} \\ + e^{2|\alpha|^2[e^{-\gamma T/2} \cos\Delta(T-t_i) - 1]}\}\}. \quad (4.14)$$

This probability exhibits a variation with T quite similar to the one displayed in Fig. 3 of Ref. [15]. When $\gamma \rightarrow 0$, we get Eq. (4.13), as expected. For finite γ , $P_{(g)}(T)$ exhibits peaks whose amplitudes decays as $\exp(-|\alpha|^2 \gamma T)$, corresponding to a lifetime $t_c/|\alpha|^2$ of the macroscopic coherence.

C. Effect of velocity dispersion

We assume that the first atom prepares the field in the state (4.7). The second atom comes a time T after the first one, with a different velocity.

Let

$$\mathcal{F}'_1 = D_1(k\alpha e^{-i\Delta T})e^{-i\Delta t'_1 a_1^\dagger a_1}, \quad (4.15a)$$

$$\mathcal{F}'_2 = D_2(k\alpha e^{i\phi_{v'}} e^{-i\Delta T})e^{-i\Delta t'_2 a_2^\dagger a_2}, \quad (4.15b)$$

where k is a real number, assumed to be close to one, and $\phi_{v'}$ is the noncompensated phase shift between the cavity mode and the source during the atom time of flight from the first to the second cavity:

$$\phi_{v'} = -\Delta \left(\frac{L}{v'} - \frac{L}{v} \right) \approx \Delta \times L \frac{\delta v}{v^2}, \quad (4.16)$$

where $\delta v = v' - v$. The probability of finding the second atom in state e or g is given by

$$P_{(e)}^{(g)} = \frac{1}{2} \{ 1 \pm \text{Re}[\text{Tr}(\mathcal{F}'_1 |\psi_F\rangle\langle\psi_F| \mathcal{F}'_2^\dagger)] \}. \quad (4.17)$$

For $|\alpha|^2 \gg 1$, and $\Delta T/\pi$ an even integer, we get

$$\text{Tr}(\mathcal{F}'_1 |\psi_F\rangle\langle\psi_F| \mathcal{F}'_2^\dagger) \approx \frac{1}{2} e^{i\psi_1} \langle \alpha, k\alpha e^{i\phi_{v'}} | k\alpha, \alpha \rangle, \quad (4.18)$$

while if $\Delta(T - t'_i)/\pi$ is an odd integer,

$$\text{Tr}(\mathcal{F}'_1 |\psi_F\rangle\langle\psi_F| \mathcal{F}'_2^\dagger) \approx \frac{1}{2} e^{-i\psi_1} \langle 0, \alpha(k e^{i\phi_{v'}} - 1) | \alpha(k-1), 0 \rangle. \quad (4.19)$$

The conditional probability (4.17) becomes then, if $|\alpha|^2 \gg 1$ and $\Delta T/\pi$ is an even integer,

$$P_{(g)}^{(e)} \approx \frac{1}{2} [1 \pm \frac{1}{2} e^{-|\alpha|^2(1-k)^2} e^{-k|\alpha|^2(1-\cos\phi_{v'})} \times \cos(\psi_1 - k|\alpha|^2 \sin\phi_{v'})], \quad (4.20)$$

while if $|\alpha|^2 \gg 1$ and $\Delta(T - t'_i)/\pi$ is an odd integer,

$$P_{(g)}^{(e)} \approx \frac{1}{2} [1 \pm \frac{1}{2} e^{-|\alpha|^2(1-k)^2} e^{-k|\alpha|^2(1-\cos\phi_{v'})} \cos\psi_1]. \quad (4.21)$$

If $\Delta T/\pi$ is an even integer, and $\Delta t'_i/\pi$ is an odd integer, we get instead

$$P_{(g)}^{(e)} \approx \frac{1}{2} \{ 1 \pm \frac{1}{2} e^{-|\alpha|^2(1-k)^2} e^{-k|\alpha|^2(1-\cos\phi_{v'})} [\cos(\psi_1 - k|\alpha|^2 \sin\phi_{v'}) + \cos\psi_1] \}. \quad (4.22)$$

In order that the peaks do not become negligible, one should satisfy, for (4.20), the conditions

$$|\alpha|^2(1-k)^2 \leq 1, \quad (4.23a)$$

$$k|\alpha|^2 \phi_{v'}^2 \leq 1, \quad (4.23b)$$

$$k|\alpha|^2 \phi_{v'} \leq 1, \quad (4.23c)$$

while for (4.21) only conditions (4.23a) and (4.23b) apply.

Since $|\alpha| \ll 1/v$, we have $|1-k| = |\Delta\alpha/\alpha| = |\delta v|/v$, and therefore (4.23a) implies that $|\alpha|^2 \leq (v/\delta v)^2$. For $\Delta v/v \approx 10^{-2}$, this means $|\alpha|^2 \leq 10^4$.

Since $\phi_{v'} = \Delta L \delta v/v^2$, and $k \approx 1$, condition (4.23b) implies that $|\alpha|^2 \leq (v/\delta v)^2 [v/(\Delta L)]^2$. However, $|\Delta|$ must be at least of the order of the transit-time-broadened linewidth of the atom, that is, $1/t'_i \leq |\Delta|$. But $t'_i \leq L/v$, so that $v/L \leq |\Delta|$ and $v/(\Delta L) \leq 1$. Therefore one should have $|\alpha|^2 \leq (v/\delta v)^2$, which coincides with the restriction coming from (4.23a).

Finally, we get from (4.23c) that $|\alpha|^2 \leq (v/\delta v) \times [v/(\Delta L)]$, or yet $|\alpha|^2 \leq v/\delta v$. For $\delta v/v \approx 10^{-2}$, this yields $|\alpha|^2 \leq 100$, which is the most restrictive condition so far. It is interesting, however, to note that this last condition applies only to the peaks associated with the condition $\Delta T/\pi$ equal to an even number. Therefore the peaks which show up whenever $\Delta(T - t'_i)/\pi$ becomes equal to an odd number are more robust with respect to the velocity spread. As this spread increases, these peaks survive the others, up to the point when conditions (4.23a) and (4.23b) are also violated.

Note finally that, as in the case of the quantum switch, a high detection efficiency is necessary, since unread atoms also spoil the quantum correlation between the two cavities.

V. CONCLUSION

Recent developments in quantum optics, including the production of long-lived circular Rydberg states, of velocity-selected atomic beams, and of high- Q superconducting cavities, have made it possible to observe phenomena which are at the heart of quantum mechanics. In this paper, we have discussed three realistic experimental arrangements, which could produce coherent superpositions of mesoscopic states of the electromagnetic field (Schrödinger cats), at the frontier between the macroscopic and the microscopic worlds, and the subsequent monitoring of their decoherence, due to dissipation. These experiments would constitute an ideal test of the measurement theory, since the classically distinguishable field states correspond to the distinct positions of a macroscopic pointer. One could thus, by monitoring the decoherence between those states, follow the ‘‘collapse’’ of the quantum state into a classical statistical mixture. Furthermore, the nonlocal state of the field discussed in Sec. IV provides an EPR-like experiment in which quantum correlations between spatially separated mesoscopic systems can be demonstrated.

The conjugation of low-dissipation cavities with the atomic correlation technique has allowed us to overcome the two usual obstacles to the realization of such experiments. Large cavity damping times yield coherence lifetimes in the observable range, for up to 100 photons in the cavity, while the probing of the coherence by the second atom is equivalent to the measurement of a nonlocal operator.

ACKNOWLEDGMENT

One of the authors (L.D.) thanks the Conselho Nacional de Desenvolvimento Científico e Tecnológico (Brazil) for support.

APPENDIX A: DISSIPATION IN THE QUANTUM SWITCH

Let us calculate the time evolution, due to dissipation, of the field density matrix corresponding to the quantum switch, as well as of the conditional probability for finding the sec-

ond atom in state g or e , after having detected the first atom in one of the two states.

The method coincides with the one adopted in Sec. II. We start from the expression for the normal-ordered characteristic function (2.11) corresponding to state (3.1):

$$C_N(\lambda, \lambda^*, 0) = \frac{1}{N_2} [e^{(\lambda \alpha^* - \lambda^* \alpha)} + 1 + e^{-|\alpha|^2/2} (e^{i\psi_1} e^{\lambda \alpha^*} + e^{-i\psi_1} e^{-\lambda^* \alpha})]. \quad (\text{A1})$$

The time evolution of this characteristic function is given by (2.13), so that

$$C_N(\lambda, \lambda^*, t) = \frac{1}{N_2} [e^{(\lambda \alpha^* - \lambda^* \alpha) e^{-\gamma t/2}} + 1 + e^{-|\alpha|^2/2} (e^{i\psi_1} e^{\lambda \alpha^* e^{-\gamma t/2}} + e^{-i\psi_1} e^{-\lambda^* \alpha e^{-\gamma t/2}})]. \quad (\text{A2})$$

This expression corresponds to the following density operator:

$$\rho_F(t) = \frac{1}{N_2} [|\alpha e^{-\gamma t/2}\rangle \langle \alpha e^{-\gamma t/2}| + |0\rangle \langle 0| + e^{-|\alpha|^2(1-e^{-\gamma t})/2} (e^{i\psi_1} |0\rangle \langle \alpha e^{-\gamma t/2}| + e^{-i\psi_1} |\alpha e^{-\gamma t/2}\rangle \langle 0|)]. \quad (\text{A3})$$

This equation clearly displays the transition from the initial pure state to the final complete statistical mixture. For $t=0$, we get the density operator corresponding to the state (3.1). When $\gamma t \ll 1$, we may approximate $\exp[-|\alpha|^2(1-e^{-\gamma t})/2] \approx \exp(-\gamma |\alpha|^2 t/2)$, so that the coherent contribution to (A3) decays with a lifetime $2t_c/|\alpha|^2$. For $2t_c/|\alpha|^2 \ll t \ll t_c$, (A3) becomes a statistical mixture, with equal weights, of the states $|0\rangle$ and $|\alpha e^{-\gamma t}\rangle$.

From (A3) and (3.5) we calculate now the conditional probability (3.17). We use that

$$\begin{aligned} \text{Tr}[\mathcal{S} \rho_F(T)] &= \frac{1}{N_2} [\langle \alpha e^{-\gamma T/2} | \mathcal{S} | \alpha e^{-\gamma T/2} \rangle + \langle 0 | \mathcal{S} | 0 \rangle + e^{-|\alpha|^2(1-e^{-\gamma T})/2} (e^{i\psi_1} \langle \alpha e^{-\gamma T/2} | \mathcal{S} | 0 \rangle + e^{-i\psi_1} \langle 0 | \mathcal{S} | \alpha e^{-\gamma T/2} \rangle)] \\ &= \frac{1}{N_2} [e^{i\phi_\alpha(T)} \langle \alpha e^{-\gamma T/2} | \alpha (e^{-i\Delta T} + e^{-\gamma T/2} e^{-i\Delta t_i}) \rangle + \langle 0 | \alpha e^{-i\Delta T} \rangle + e^{-|\alpha|^2[1-e^{-\gamma T}]/2} [e^{i\psi_1} \langle \alpha e^{-\gamma T/2} | \alpha e^{-i\Delta T} \rangle \\ &\quad + e^{i\phi_\alpha(T)} e^{-i\psi_1} \langle 0 | \alpha (e^{-i\Delta T} + e^{-\gamma T/2} e^{-i\Delta t_i}) \rangle]], \end{aligned} \quad (\text{A4})$$

where $\phi_\alpha(T)$ is given by

$$\phi_\alpha(T) = |\alpha|^2 e^{-\gamma T/2} \sin[\Delta(t_i - T)]. \quad (\text{A5})$$

Writing down the expressions for the scalar products, we get explicitly

$$\begin{aligned} \text{Tr}(\mathcal{S} \rho_F) &= \frac{e^{-|\alpha|^2/2}}{2N_2} \{ e^{-|\alpha|^2[(1-e^{-i\Delta t_i})e^{-\gamma t} - e^{-i\Delta T} e^{-\gamma t/2} + e^{i\Delta(T-t_i)} e^{-\gamma t/2}]} \\ &\quad + 1 + e^{-|\alpha|^2/2} [e^{i\psi_1} e^{|\alpha|^2 e^{-\gamma t/2} e^{-i\Delta T}} \\ &\quad + e^{-i\psi_1} e^{-|\alpha|^2 e^{-\gamma t/2} e^{i\Delta(T-t_i)}]} \}. \end{aligned} \quad (\text{A6})$$

The first two terms on the right-hand side of (A6) give negligible contributions when $|\alpha|^2 \gg 1$. Replacing the remaining contributions in (3.17), we obtain expression (3.18).

APPENDIX B: DISSIPATION IN A NONLOCAL FIELD

We consider here the two-cavity system, and calculate the time evolution of the field density operator, due to dissipa-

tion, as well as the time-dependent conditional probability of finding the second atom in the same or in a different state than the first one.

The initial field density operator is obtained from (4.7):

$$\rho_F(0) = \frac{1}{N_3} [|\alpha, 0\rangle \langle \alpha, 0| + |0, \alpha\rangle \langle 0, \alpha| + (e^{i\psi_1} |0, \alpha\rangle \langle \alpha, 0| + e^{-i\psi_1} |\alpha, 0\rangle \langle 0, \alpha|)]. \quad (\text{B1})$$

From this expression, we get the normal-ordered characteristic function right after the preparation of the state:

$$\begin{aligned} C_N(\lambda_1, \lambda_2; \lambda_1^*, \lambda_2^*; 0) &= \text{Tr}[\rho_F(t) e^{\lambda_1 a_1^\dagger} e^{\lambda_2 a_2^\dagger} e^{-\lambda_1^* a_1} e^{-\lambda_2^* a_2}] \\ &= \frac{1}{N_3} \{ e^{(\lambda_1 \alpha^* - \lambda_1^* \alpha)} + e^{(\lambda_2 \alpha^* - \lambda_2^* \alpha)} \\ &\quad + e^{-|\alpha|^2} [e^{i\psi_1} e^{(\lambda_1 \alpha^* - \lambda_2^* \alpha)} + e^{-i\psi_1} e^{(\lambda_2 \alpha^* - \lambda_1^* \alpha)}] \}. \end{aligned} \quad (\text{B2})$$

As before, the time evolution of this characteristic function is obtained from

$$C_N(\lambda_1, \lambda_2; \lambda_1^*, \lambda_2^*; t) = C_N(\lambda_1 e^{-\gamma t/2}, \lambda_2 e^{-\gamma t/2}; \lambda_1^* e^{-\gamma t/2}, \lambda_2^* e^{-\gamma t/2}; 0), \quad (\text{B3})$$

so that

$$C_N(\lambda_1, \lambda_2; \lambda_1^*, \lambda_2^*; t) = \frac{1}{N_3^2} \{ e^{(\lambda_1 \alpha^* - \lambda_1^* \alpha) e^{-\gamma t/2}} + e^{(\lambda_2 \alpha^* - \lambda_2^* \alpha) e^{-\gamma t/2}} + e^{-|\alpha|^2} [e^{i\psi_1} e^{(\lambda_1 \alpha^* - \lambda_2^* \alpha) e^{-\gamma t/2}} + e^{-i\psi_1} e^{(\lambda_2 \alpha^* - \lambda_2^* \alpha) e^{-\gamma t/2}}] \}. \quad (\text{B4})$$

This expression for the characteristic function corresponds to the following density operator:

$$\rho_F(t) = \frac{1}{N_3^2} [|\alpha e^{-\gamma t/2}, 0\rangle \langle \alpha e^{-\gamma t/2}, 0| + |0, \alpha e^{-\gamma t/2}\rangle \langle 0, \alpha e^{-\gamma t/2}| + e^{-|\alpha|^2(1-e^{-\gamma t})} (e^{i\psi_1} |0, \alpha e^{-\gamma t/2}\rangle \langle \alpha e^{-\gamma t/2}, 0| + e^{-i\psi_1} | \alpha e^{-\gamma t/2}, 0\rangle \langle 0, \alpha e^{-\gamma t/2}|)]. \quad (\text{B5})$$

This expression exhibits explicitly the transformation of the initial pure state into a statistical mixture. While the intensity lifetime is t_c , we see that for $|\alpha|^2 \ll \gamma t \ll 1$, the coherences vanish with a lifetime equal to $t_c/|\alpha|^2$, two times smaller than in the quantum switch case.

From (B5), (4.8), and (4.9), we get

$$\text{Tr}[\mathcal{S}_1 \rho_F(T) \mathcal{S}_2^\dagger] = \frac{1}{N_3^2} \{ \langle \alpha e^{-\gamma T/2} | \alpha (e^{-i\Delta T} + e^{-\gamma T/2} e^{-i\Delta t_i}) \rangle \langle \alpha e^{-i\Delta T} | 0 \rangle e^{i\phi_\alpha(T)} + \langle 0 | \alpha e^{-i\Delta T} \rangle \langle \alpha (e^{-i\Delta T} + e^{-\gamma T/2} e^{-i\Delta t_i}) | \alpha e^{-\gamma T/2} \rangle e^{-i\phi_\alpha(T)} + e^{-|\alpha|^2(1-e^{-\gamma T})} [e^{i\psi_1} \langle \alpha e^{-\gamma T/2} | \alpha e^{-i\Delta T} \rangle \langle \alpha e^{-i\Delta T} | \alpha e^{-\gamma T/2} \rangle + e^{-i\psi_1} \langle 0 | \alpha (e^{-i\Delta T} + e^{-\gamma T/2} e^{-i\Delta t_i}) \rangle \langle \alpha (e^{-i\Delta T} + e^{-\gamma T/2} e^{-i\Delta t_i}) | 0 \rangle] \}, \quad (\text{B6})$$

where $\phi_\alpha(T)$ is given by (A5).

For $|\alpha|^2 \gg 1$, the first two terms will always be negligible. Note that, for $t=0$, the first factor of the first term could be equal to one if $\Delta T = \pm \pi/3$ and $\Delta t_i = \mp \pi/3$ (modulo 2π), as seen in the quantum switch model. However, in this case the second factor of the first term will be much smaller than one, so that here the first term on the right-hand side of (B6) will always be negligible when $|\alpha|^2 \gg 1$. In this limit, replacing (B6) in (4.11) yields expression (4.14).

-
- [1] E. Schrödinger, *Naturwissenschaften* **23**, 807 (1935); **23**, 823 (1935); **23**, 844 (1935). English translation by J. D. Trimmer, *Proc. Am. Phys. Soc.* **124**, 3235 (1980).
- [2] Letter from Albert Einstein to Max Born in 1954, cited by E. Joos, in *New Techniques and Ideas in Quantum Measurement Theory*, edited by D. M. Greenberger (New York Academy of Science, New York, 1986); see also W. H. Zurek, S. Habib, and J. P. Paz, *Phys. Rev. Lett.* **70**, 1187 (1993).
- [3] E. Wigner, in *The Scientist Speculates*, edited by I. J. Good (William Heinemann, London, 1962), p. 284; and also in *Symmetries and Reflections* (Indiana University Press, Bloomington, 1967), p. 171; G. Ludwig, *Werner Heisenberg und die Physik unserer Zeit* (Friedrich Vieweg und Sohn, Braunschweig, 1961). See also E. Wigner, *Am. J. Phys.* **31**, No. 1 (1963).
- [4] H. Dekker, *Phys. Rev. A* **16**, 2126 (1977); A. O Caldeira and A. J. Leggett, *Physica (Amsterdam)* **121A**, 587 (1983); *Phys. Rev. A* **31**, 1059 (1985).
- [5] H. D. Zeh, *Found. Phys.* **1**, 69 (1970); W. H. Zurek, *Phys. Rev. D* **24**, 1516 (1981); **26**, 1862 (1982); W. G. Unruh and W. H. Zurek, *ibid.* **40**, 1071 (1989); W. H. Zurek, *Phys. Today* **44** (10), 36 (1991); B. L. Hu, J. P. Paz, and Y. Zhang, *Phys. Rev. D* **45**, 2843 (1992).
- [6] J. von Neumann, *Die Mathematische Grundlagen der Quantenmechanik* (Springer-Verlag, Berlin, 1932); English translation by R. T. Beyer: *Mathematical Foundations of Quantum Mechanics* (Princeton University Press, Princeton, NJ, 1955).
- [7] *Quantum Theory and Measurement*, edited by J. A. Wheeler and W. H. Zurek (Princeton University Press, Princeton, NJ, 1983); W. Zurek, *Phys. Today* **44** (10), 36 (1991); R. Omnès, *The Interpretation of Quantum Mechanics* (Princeton University Press, Princeton, NJ, 1994).
- [8] K. Hepp, *Helv. Phys. Acta* **45**, 237 (1972); K. Hepp and E. H. Lieb, *ibid.* **46**, 573 (1973); J. S. Bell, *ibid.* **48**, 93 (1975).
- [9] E. Joos and H. D. Zeh, *Z. Phys. B* **59**, 223 (1985); G. J. Milburn and C. A. Holmes, *Phys. Rev. Lett.* **56**, 2237 (1986); F. Haake and D. Walls, *Phys. Rev. A* **36**, 730 (1987).
- [10] K. Gottfried, *Quantum Mechanics* (Benjamin, Reading, MA, 1966), Sec. IV.
- [11] A. J. Leggett, *Quantum Mechanics at the Macroscopic Level in Chance and Matter*, Les Houches Summer School, session XLVI, edited by J. Souletie, J. Vannimenus, and R. Stora (North-Holland, Amsterdam, 1987), p. 395.
- [12] B. Yurke and D. Stoler, *Phys. Rev. Lett.* **57**, 13 (1986); B. Yurke, W. Schleich, and D. F. Walls, *Phys. Rev. A* **42**, 1703 (1990); G. Milburn, *ibid.* **33**, 674 (1986); C. M. Savage, S. L. Braunstein, and D. F. Walls, *Opt. Lett.* **15**, 628 (1990).
- [13] M. Brune, S. Haroche, J. M. Raimond, L. Davidovich, and N. Zagury, *Phys. Rev. A* **45**, 5193 (1992).
- [14] J. S. Bell, *Physics (Long Island City, N. Y.)* **1**, 195 (1964).

- [15] L. Davidovich, A. Maali, M. Brune, J. M. Raimond, and S. Haroche, Phys. Rev. Lett. **71**, 2360 (1993); see also S. Haroche, M. Brune, J.-M. Raimond, and L. Davidovich, in *Fundamentals of Quantum Optics III*, edited by F. Ehlotzky (Springer-Verlag, Amsterdam, 1993).
- [16] R. J. Glauber, Phys. Rev. **130**, 2529 (1963); **131**, 2766 (1963); also in *Quantum Optics and Electronics*, Les Houches 1964 Summer School, edited by C. DeWitt, A. Blandin, and C. Cohen-Tannoudji (Gordon and Breach, New York, 1965).
- [17] R. G. Hulet and D. Kleppner, Phys. Rev. Lett. **51**, 1430 (1983); A. Nussenzveig *et al.*, Europhys. Lett. **14**, 755 (1991).
- [18] M. Brune, P. Nussenzveig, F. Schmidt-Kaler, F. Bernardot, A. Maali, J. M. Raimond, and S. Haroche, Phys. Rev. Lett. **72**, 3339 (1994).
- [19] N. F. Ramsey, *Molecular Beams* (Oxford University Press, New York, 1985).
- [20] A. Einstein, B. Podolski, and N. Rosen, Phys. Rev. **47**, 777 (1935).
- [21] S. J. Freedman and J. S. Clauser, Phys. Rev. Lett. **28**, 938 (1972); A. Aspect, J. Dalibard, and G. Roger, *ibid.* **49**, 1804 (1982).
- [22] W. H. Louisell and W. H. Marburger, IEEE J. Quantum Electron. **3**, 348 (1967).
- [23] J. Perina, *Quantum Statistics of Linear and Non Linear Optical Phenomena* (Reidel, Dordrecht, 1984).
- [24] P. Meystre, in *Progress in Optics XXX*, edited by E. Wolf (Elsevier Science, New York, 1992); L. Davidovich, N. Zagury, M. Brune, J. M. Raimond, and S. Haroche, Phys. Rev. **50**, R895 (1994).